[15] T. Kurien, "Issues in the design of practical multitarget tracking algorithms," in *Multisensor-Multitarget Tracking: Applications and Advances*, Y. Bar-Shalom, Ed. Boston, MA: Artech House, 1990, vol. 1, ch. 3, reprinted by YBS Publishing, 1998.
[16] M. Levedahl, "Performance comparison of 2-D assignment algorithms for assigning truth objects to measured tracks," in *Proc. SPIE: Signal Data Process. Small Targets Conf.*, Jul. 2000, vol. 4048, pp. 380–389.
[17] D. B. Reid, "An algorithm for tracking multiple targets," *IEEE Trans. Autom. Control*, vol. AC-24, no. 6, pp. 843–854, Dec. 1979.
[18] D. Schuhmacher, B.-T. Vo, and B.-N. Vo, "A consistent metric for performance evaluation of multi-object filters," *IEEE Trans. Signal Process.*, vol. 56, no. 8, pp. 3447–3457, Aug. 2008.
[19] D. Svensson, "Target Tracking in Complex Scenarios," Ph.D. dissertation, Chalmers Univ. of Technology, Göteborg, Sweden, 2010, pp. 111–146.
[20] L. Svensson, D. Svensson, M. Guerriero, and P. Willett, "Set JPDA algorithm for multi-target tracking," *IEEE Trans. Signal Process.*, 2010, submitted for publication.

Joint Initialization and Tracking of Multiple Moving Objects Using Doppler Information

Ju Hong Yoon, Du Yong Kim, Seung Hwan Bae, and Vladimir Shin

***Abstract*—In this correspondence, a new multi-target tracking (MTT) algorithm based on the probability hypothesis density (PHD) filtering framework is designed in order to improve tracking performance via the proposal of two contributions. First, unlike typical existing systems, Doppler information is additionally employed to enhance the clutter rejection capability. Specifically, position and Doppler measurements are iteratively incorporated in a two-step process based on a Gaussian mixture PHD (GMPHD) filter. Second, a concrete initialization process is proposed in the birth intensity design of the GMPHD. The initialization process from consecutive measurements leads to a reliable birth intensity that improves track management performance. Both contributions are subsequently evaluated through MTT simulations, the results of which verify that the proposed algorithm is viable.**

***Index Terms*—Bayesian filtering, Doppler information, initialization, multi-target tracking, PHD filter.**

I. Introduction

A reliable multi-target tracking (MTT) filter requires a sufficient reduction of measurement uncertainties and efficient track management. Measurements obtained from radar, sonar, or laser sensors contain uncertainties; such as random measurement error, spurious returns from clutter, detection loss, etc. Based on these measurements, the purpose of the MTT filter is to estimate a set of multiple target states. Simultaneously, the number of targets should be known in order to ensure efficient track management and to resolve the appearance and disappearance of targets [1]–[3].

In literature, the two challenges of MTT mentioned above are usually discussed by attempting to develop data association algorithms that correctly assign target-oriented measurements and exclude clutter-oriented measurements. Among them, common algorithms include multiple hypotheses tracking (MHT), probabilistic data association (PDA), joint probabilistic data association (JPDA) and their extended versions with additional track management [2]–[7]. However, existing algorithms require that independent blocks (single tracker, data association and track management) be combined in order to implement the MTT filter. This approach can significantly increase the computational load of the filter especially when the number of targets increases as time evolves [3], [8].

Recently, as an alternative approach, a probability hypothesis density (PHD) filter has been proposed which avoids the data association between measurements and includes clutter rejection in a unified framework via finite set statistics and Bayesian analysis [3], [8]. There have been two main implementations of the PHD: the first is based on using the sequential Monte Carlo method (i.e., SMCPHD) and the other uses a Gaussian mixture representation (GMPHD). Note that GMPHD is a unique closed form implementation of a PHD filter. And it is computationally efficient compared to the SMCPHD in linear dynamic systems because only dominant Gaussian components are needed to be preserved [9]–[11].

In the MTT problem, position measurements are typically utilized to estimate both the current position and the number of targets. To enhance the performance of MTT filters, information such as amplitude information (AI) [12]–[14] and Doppler information (DI) [15]–[17] can be further considered. In contrast to the sole use of position measurements, AI or DI could improve the data association. In this work, to improve the performance of the GMPHD filter, we focus on the usage of DI to attain three benefits: 1) rejection of clutter-oriented measurements, 2) more efficient measurement update step, and 3) provision of initial target velocities using only a one-step measurement.

As opposed to AI, DI contains kinematic information related to the target state because it originates from the target's velocity, thereby it can be effectively used to correct target states especially for the target velocity. In addition, the initial velocity information of newly appearing targets can be obtained from the DI that helps the track initialization. If the DI is not provided, the initial velocity of new targets at time instant k is usually assumed to be normally distributed with zero mean and a chosen variance based on the maximum target speed. In this case, as the variance becomes larger, inaccuracies in the initial states of the new targets become worse. Consequently, this condition leads to a track initialization failure in the next step. Note that though a two-step initialization (i.e., TSI also called a "two-point initiation") may be used as an alternative, it consumes additional computational resources [16].

In this correspondence, we present two main contributions that have yet to be discussed in GMPHD. First, we focus on track initiation and tracking multiple moving targets associated with GMPHD filtering via an initialization step using consecutive measurements whereas the birth target components designed by using arbitrary mean and covariance in the standard GMPHD filter fail to calculate the gradient of Doppler measurement function properly in the update step. Second, the DI is incorporated for more precise birth target selection and improving the

Manuscript received October 11, 2010; revised January 13, 2011 and February 22, 2011; accepted March 08, 2011. Date of publication March 24, 2011; date of current version June 15, 2011. The associate editor coordinating the review of this manuscript and approving it for publication was Prof. Maciej Niedziecki. This work was supported by Basic Science Research Program through the National Research Foundation of Korea (NRF) funded by the Ministry of Education, Science and Technology (no. 2011-0004475).

J. H. Yoon, D. Y. Kim, and S. H. Bae are with the School of Information and Communications, Gwangju Institute of Science and Technology, Gwangju 500-712, South Korea (e-mail: jhyoon@gist.ac.kr; duyong@gist.ac.kr; bshwan@gist.ac.kr).

V. Shin was with the School of Mechatoronics, Gwangju Institute of Science and Technology, Gwangju, South Korea. He is now with the Department of Information and Statistics, Gyeongsang National University, Jinju 660-701, South Korea (e-mail: vishin@gnu.ac.kr).

Color versions of one or more of the figures in this correspondence are available online at http://ieeexplore.ieee.org.

Digital Object Identifier 10.1109/TSP.2011.2132720

accuracy of predicted states. Considering these two contributions, we denote our algorithm as the GMPHD with initialization and Doppler information, i.e., GMPHD-I-DI.

The remainder of the correspondence is organized as follows. Section II presents the problem formulation. In Section III, the GMPHD-I-DI filter is proposed and we briefly present the GMPHD-I filter when DI is not available. In Section IV, we introduce an efficient track initialization algorithm based on one step initialization (OSI) procedure using DI. In Section V, performance of the GMPHD-I-DI filter is presented through an MTT simulation scenario and a comparison with other filters in terms of estimation accuracy of multiple target positions and number of targets is given.

II. Problem Formulation

We present a dynamic system model of multiple moving targets based on random finite set (RFS) formulation and a measurement system model containing the angle, range and DI from targets, clutter and false alarms.

Each target state at time k is denoted as $x_k^{(i)} = [p_{X,k}^{(i)}, \dot{p}_{X,k}^{(i)}, p_{Y,k}^{(i)}, \dot{p}_{Y,k}^{(i)}]^T$, $i = 1, \ldots, N_k$, where $p_{X,k}^{(i)}$ and $p_{Y,k}^{(i)}$ are x and y coordinate positions, respectively, $\dot{p}_{X,k}^{(i)}$ and $\dot{p}_{Y,k}^{(i)}$ are the corresponding velocities, N_k is the number of targets and is time-varying because existing targets may disappear or continue to survive and new targets may appear at any time. As such, the multiple target states at time $k-1$ are expressed by the RFS $X_{k-1} = \left\{x_{k-1}^{(1)}, \ldots, x_{k-1}^{(N_{k-1})}\right\}$. Here, the cardinality of RFS X_{k-1} changes according to the survival probability $p_{S,k}(x_{k-1})$ and the death probability $1 - p_{S,k}(x_{k-1})$ of each target $x_{k-1} \in X_{k-1}$ in the next time step k. In this case, the time evolution of the RFS X_{k-1} can be modeled as [9], [10]

$$X_k = \left[\bigcup_{x_k \in X_{k-1}} S_{k|k-1}(x_k)\right] \cup \Gamma_k \tag{1}$$

where $\bigcup_{x_k \in X_{k-1}} S_{k|k-1}(x_k)$ is the survival target RFS at time k based on RFS X_{k-1} at the previous time and Γ_k represents birth target RFS. Trajectories of all surviving and birth targets are assumed to follow a discrete-time linear dynamic model:

$$x_k = F x_{k-1} + w_{k-1},\ x_k \in X_k \tag{2}$$

where F is the transition matrix and $w_k \in \Re^4 \sim N(w_k; 0, Q_k)$ is white Gaussian noise with covariance Q_k and $E\left(w_i w_j^T\right) = 0,\ i \neq j$ [19].

We assume that measurements of surviving and birth targets are obtained at time k, with the probability of detection being $p_D < 1$. Measurements include the angle, range and DI for each target. Such measurements consist of the RFS of the detected target-oriented measurements $\Theta_k(x_k), x_k \in X_k$ and the RFS of clutter-oriented measurements K_k. Thus, all available measurements can be expressed by the RFS $Z_k = \left\{z_k^{(l)}, \ldots, z_k^{(M_k)}\right\}$ [9], [10]:

$$Z_k = \left[\bigcup_{x \in X_k} \Theta_k(x_k)\right] \cup K_k. \tag{3}$$

We assume that the sensor is stationary and located at (0, 0) in the Cartesian plane and then, each target-oriented measurement $z_k \in \Theta_k(x_k)$ can be obtained by

$$z_k = [\, z_{r,k} \quad z_{\theta,k} \quad z_{d,k}\,]^T = h_k(x_k) + \xi_k,\ z_k \in \Theta_k(x_k) \tag{4}$$

$$h_k(x_k) = \begin{bmatrix} h_r(x_k) \\ h_\theta(x_k) \\ h_d(x_k) \end{bmatrix} = \begin{bmatrix} r_k \\ \theta_k \\ d_k \end{bmatrix} = \begin{bmatrix} \sqrt{p_{x,k}^2 + p_{y,k}^2} \\ \tan^{-1}\left(\frac{p_{y,k}}{p_{x,k}}\right) \\ -\dot{p}_{x,k}\cos(\theta_k) - \dot{p}_{y,k}\sin(\theta_k) \end{bmatrix} \tag{5}$$

where r_k, θ_k and d_k are the range, angle and DI, respectively and $\xi_k \in \Re^3 \sim N(\xi_k; 0, R_k)$ is white Gaussian noise with covariance $R_k = diag[\,\sigma_r^2 \quad \sigma_\theta^2 \quad \sigma_d^2\,]$ and $E\left(\xi_i \xi_j^T\right) = 0, i \neq j$. We assume that w_k and ξ_k are uncorrelated.

III. GMPHD-I-DI Filter

The GMPHD-I-DI filter is based on a GMPHD filter; i.e., the theoretical basis of both filters is identical. Adopting the GM form, the GMPHD approximates the full posterior density (as in an optimal Bayesian filter) to significantly reduce the computational complexity for online processing [3], [10].

Following the GM approximation, a posterior intensity at time $k-1$ takes the form:

$$v_{k-1}(x) = \sum_{j=1}^{J_{k-1}} w_{k-1}^{(j)} N\left(x; m_{k-1}^{(j)}, P_{k-1}^{(j)}\right) \tag{6}$$

where J_{k-1} is the number of Gaussian components, i.e., mean $m_{k-1}^{(j)}$ and covariance $P_{k-1}^{(j)}$. Then, the prediction value of $v_{k-1}(x)$ represents the sum of the two prediction intensities

$$\begin{aligned} v_{k|k-1}(x) &= v_{S,k|k-1}(x) + \gamma_k(x) \\ &= \sum_{j=1}^{J_{k|k-1}} w_{k|k-1}^{(j)} N\left(x; m_{k|k-1}^{(j)}, P_{k|k-1}^{(j)}\right), \end{aligned} \tag{7}$$

$$\begin{aligned} v_{S,k|k-1}(x) &= \sum_{j=1}^{J_{k-1}} p_{S,k}(x)\, w_{k-1}^{(j)} N\left(x; m_{S,k|k-1}^{(j)}, P_{S,k|k-1}^{(j)}\right), \\ \left[m_{S,k|k-1}^{(j)}, P_{S,k|k-1}^{(j)}\right] &= \mathrm{KF\_P}\left(m_{k-1}^{(j)}, P_{k-1}^{(j)}, F, Q_k\right), \end{aligned} \tag{8}$$

$$\begin{aligned} \gamma_k(x) &= \sum_{j=1}^{J_{\gamma,k}} p_{S,k}(x)\, w_{\gamma,k-1}^{(j)} N\left(x; m_{\gamma,k|k-1}^{(j)}, P_{\gamma,k|k-1}^{(j)}\right), \\ \left[m_{\gamma,k|k-1}^{(j)}, P_{\gamma,k|k-1}^{(j)}\right] &= \mathrm{KF\_P}\left(m_{\gamma,k-1}^{(j)}, P_{\gamma,k-1}^{(j)}, F, Q_k\right) \end{aligned} \tag{9}$$

where $v_{S,k|k-1}(x)$ is the predicted intensity of the surviving target, $\gamma_k(x)$ is the birth target intensity and $J_{k|k-1} = J_{k-1} + J_{\gamma,k}$ is the predicted number of GMs, which includes surviving and birth target intensities. The predicted components $\left(m_{S,k|k-1}^{(j)}, P_{S,k|k-1}^{(j)}\right)$ of the surviving target are obtained via Kalman filter (KF) prediction, i.e., 'KF_P'. Unlike typical PHD implementations, however, we incorporate an initialization step into the birth target intensity by applying the KF prediction to the initial birth target components $\left(m_{\gamma,k-1}^{(j)}, P_{\gamma,k-1}^{(j)}\right)$ obtained by OSI, TSI [16]–[18], or the algorithm specified in Section IV when the DI is available. The standard GMPHD has the birth target intensity with user-defined components (arbitrary means and covariances), with which we cannot compute the gradient of the Doppler measurement function properly. On the contrary, our method utilizes the components obtained from the initialization

method followed by the KF prediction. Therefore, the proposed method suggests adaptive and automatic birth intensity of GMPHD.

In this correspondence, to update multiple target states using the polar coordinate measurements with the standard KF, we convert polar coordinate to Cartesian coordinate measurements via the relations $z_{X,k} = \lambda_\theta^{-1} z_{r,k} \cos(z_{\theta,k})$ and $z_{Y,k} = \lambda_\theta^{-1} z_{r,k} \sin(z_{\theta,k})$ using a bias compensation factor $\lambda_\theta = \exp\left(\frac{\sigma_\theta^{-2}}{2}\right)$ [20]. The set of converted measurements $Y_{C,k}$ and their corresponding Doppler measurements, D_k, is then denoted as RFS $Z_{C,k} = [Y_{C,k}; D_k] = \left[z_{C,k}^{(1)}, \ldots, z_{C,k}^{(M_k)}\right]$, where M_k is the number of measurements and $z_{C,k}^{(m)} = [\, z_{X,k}^{(m)} \quad z_{Y,k}^{(m)} \quad z_{d,k}^{(m)} \,]^T, m = 1, \ldots, M_k$.

Hence, the updated posterior intensity $v_k(x)$ is given by

$$v_k(x) = (1 - p_D)\, v_{k|k-1}(x) + \sum_{z_C \in Z_{C,k}} \sum_{j=1}^{J_{k|k-1}} w_k^{(j)}(z_C)\, N\left(x; m_{k|k}^{(j)}(z_C), P_{k|k}^{(j)}(z_C)\right). \quad (10)$$

To effectively associate DI in GMPHD, we propose a three-step procedure. In the first step, we update the predicted components $\left(m_{k|k-1}^{(j)},\ P_{k|k-1}^{(j)}\right)$ with the KF using the converted position measurement, $y_C \in Y_{C,k}$ to obtain the tentative tracks. After that, we update target states using the corresponding DI $d_k \in D_k$, in the second step with the extended KF. The advantage of this consideration is that it can calculate the gradient of the Doppler measurement function (15) more accurately because we create the tentative tracks from the position update followed by the corresponding DI update; it gives us more efficient results than updating using augmented measurement approach [15] in performance. When the augmented measurements are used, the gradient of Doppler function is computed using each erroneous predicted target state. However, in our method, the errors of target states are reduced by updating position measurements and then the corrected target states are used to calculate the gradient of the Doppler function. Moreover, the errors in birth target components from the initialization step also can be efficiently lessened by the position measurement update. The similar idea is recently introduced in [17] but it is limited to the single target tracking framework. In this correspondence, this idea is extended to the GMPHD framework as we propose from Step 1 to 3. The one iteration of Step 1 to 3 is done for each measurement, $z_{C,k}^{(m)},\ m = 1, \ldots, M_k$.

Step 1: *Updating target states using converted position measurements* $y_C = [\, z_X^{(m)} \quad z_Y^{(m)} \,]^T$.

For this purpose, we use the Kalman filter update denoted as "KF_U", such that

$$\left[m_{k|k}^{(j)}(y_C), P_{k|k}^{(j)}(y_C)\right] = \mathrm{KF\_U}\left(y_C, m_{k|k-1}^{(j)}, P_{k|k-1}^{(j)}, H, R_k(y_C)\right) \quad (11)$$

where $H = \begin{bmatrix} 1 & 0 & 0 & 0 \\ 0 & 0 & 1 & 0 \end{bmatrix}$ is the measurement matrix for converted measurements and $R_k(y_C)$ is the converted measurement error covariance obtained by using corresponding polar measurements and their covariances, σ_r^2 and σ_θ^2, based on [20, eq. (7a–7c)].

Step 2: *Updating target states using DI* $z_d = z_d^{(m)}$.

The obtained components $\left(m_{k|k}^{(j)}(y_C),\ P_{k|k}^{(j)}(y_C)\right)$ are updated using DI, such that

$$m_{k|k}^{(j)}(z_C) = m_{k|k}^{(j)}(y_C) + \Phi_{d,k}^{(j)}(y_C)\left[z_d - \hat{d}_k^{(j)}\right], \quad (12)$$

$$P_{k|k}^{(j)}(z_C) = \left(I - \Phi_{d,k}^{(j)}(y_C)\, \nabla h_{d,k}^{(j)}(y_C)\right) P_{k|k}^{(j)}(y_C), \quad (13)$$

$$\Phi_{d,k}^{(j)}(y_C) = P_{k|k}^{(j)}(y_C)\, \nabla h_{d,k}^{(j)T}(y_C) \times \left(\nabla h_{d,k}^{(j)}(y_C)\, P_{k|k}^{(j)}(y_C)\, \nabla h_{d,k}^{(j)T}(y_C) + \sigma_d^2\right)^{-1}, \quad (14)$$

$$\nabla h_{d,k}^{(j)}(y_C) = -[\, h_1 \quad h_2 \quad h_3 \quad h_4 \,],$$

$$h_1 = \frac{\dot{p}_{X,k|k}^{(j)}(y_C) + \hat{d}_k \cos\hat{\theta}_k}{\hat{r}_k},\ h_2 = \cos\hat{\theta}_k,$$

$$h_3 = \frac{\dot{p}_{Y,k|k}^{(j)}(y_C) + \hat{d}_k \sin\hat{\theta}_k}{\hat{r}_k},\ h_4 = \sin\hat{\theta}_k,$$

$$\hat{r}_k = h_r\left(m_{k|k}^{(j)}(y_C)\right),\ \hat{\theta}_k = h_\theta\left(m_{k|k}^{(j)}(y_C)\right),$$

$$\hat{d}_k = h_d\left(m_{k|k}^{(j)}(y_C)\right)$$

$$m_{k|k}^{(j)}(y_C) = \left[p_{X,k|k}^{(j)}(y_C),\ \dot{p}_{X,k|k}^{(j)}(y_C),\ p_{XY,k|k}^{(j)}(y_C),\ \dot{p}_{Y,k|k}^{(j)}(y_C)\right]^T. \quad (15)$$

Step 3: *Updating weights using measurement* $\left[z_X^{(m)}\ z_Y^{(m)}\ z_d^{(m)}\right]^T = z_C \in Z_{C,k}$.

Updated intensity weights $w_k^{(j)}(z_C)$ are calculated by

$$w_k^{(j)}(z_C) = \frac{p_D\, w_{k|k-1}^{(j)} q_k^{(j)}(y_C)\, q_k^{(j)}(z_d)}{\kappa_k(y_C)\, c(z_d) + p_D \sum_{l=1}^{J_{k|k-1}} w_{k|k-1}^{(l)} q_k^{(l)}(y_C)\, q_k^{(l)}(z_d)},$$

$$z_C = \begin{bmatrix} y_C \\ z_d \end{bmatrix} \quad (16)$$

where $q_k^{(j)}(y_C) = N\left(y_C;\ H m_{k|k-1}^{(j)},\ H P_{k|k-1}^{(j)} H^T + R_k(y_C)\right)$ and $q_k^{(j)}(z_d) = N\left(z_d\ ;\ h_d\left(m_{k|k}^{(j)}(y_C)\right),\ \nabla h_{d,k}^{(j)}(y_C)\, P_{k|k}^{(j)}(y_C)\, \nabla h_{d,k}^{(j)T}(y_C) + \sigma_d^2\right)$ represent the position and Doppler likelihood functions, respectively. In (16), the Doppler clutter intensity is $c(z_d) = N\left(z_d; 0, \sigma_d^2\right)$ for stationary clutter or we can select $c(z_d) = \frac{1}{2v_{\max}}$ by assuming the clutter speed is uniformly distributed within the interval $[-v_{\max} v_{\max}]$, where $v_{\max}$ is the maximum speed that the sensor can detect. Here, the spatial clutter intensity $\kappa_k(y_C) = \frac{m_c}{V}$ is approximately selected by considering the volume of the sensor detection range V and the average number of clutter m_c at each time (scan).

Remark 1: If the DI is not available, the update stage only includes Step 1 and 3. In this case, the updated Gaussian components $\left(m_{k|k}^{(j)}(z_C), P_{k|k}^{(j)}(z_C)\right)$ are obtained by $m_{k|k}^{(j)}(z_C) = m_{k|k}^{(j)}(y_C)$ and $P_{k|k}^{(j)}(z_C) = P_{k|k}^{(j)}(y_C)$ and, in Step 3, $q_k^{(j)}(z_d) = 1$ and $c(z_d) = 1$. We refer to this filter as the GMPHD-I filter, i.e., a combination of GMPHD and OSI (or TSI) without DI.

Remark 2: In GMPHD, the number of GM components increases exponentially as time evolves. For this problem, the removal and merging steps have been suggested in [10], [22]. To obtain the efficient GM representation of the posterior intensity $v_k(x)$, we apply the method based on the mixture weights $w_k^{(j)}(z_C)$ as given in [10]. The parameters used in the removal and merging step and the multiple target state extraction are the same as in [10]. We denote $\hat{X}_k$ as the set of extracted target states at time k, i.e., $\hat{X}_k = \left\{\tilde{m}_{e,k}^{(j)}\right\},\ j = 1, \ldots, J_{e,k}$, where $J_{e,k}$ is the number of extracted targets.

IV. One Step Initialization for GMPHD Filter Using DI

In this section, we propose adaptive birth target intensity by using the OSI method to select the intensity components. Before initializing the birth target components, we remove measurements located near the

current multi-target states $\hat{X}_k$ because measurements near $\hat{X}_k$ are not likely being obtained from the birth targets.

Part 1. Removing measurements near current multi-target states $\hat{X}_k$:

Given $\hat{X}_k$, $Y_{C,k}$, Z_k,

$$\Psi_k^{(i,j)} = \left\| H\tilde{m}_{e,k}^{(i)} - y_{C,k}^{(j)} \right\|,\ i = 1,\ldots,J_{e,k},\ j = 1,\ldots,N_k, \quad (17)$$

$Y_{b,k} := \emptyset$, $Z_{b,k} := \emptyset$

for $i = 1,\ldots,J_{e,k}$; for $j = 1,\ldots,N_k$

$$\text{if } \Psi_k^{(i,j)} > \tau,\ Y_{b,k} := Y_{b,k} \cup y_{C,k}^{(j)},\ Z_{b,k} := Z_{b,k} \cup z_k^{(j)}. \quad (18)$$

end; end

Threshold τ, i.e., a distance value, is selected according to the range standard deviation σ_r because if the measurement is target-oriented, the measurement may be located within the range standard deviation with high probability. Cardinalities of $Y_{b,k}$ and $Z_{b,k}$ are equal to $J_{\gamma,k}$ which is the number of birth target components. Components of birth targets are obtained in Part 2. When DI is not available, Part 2 is replaced by OSI or TSI [17], [18].

Part 2 : Initializing birth target components: Based on $Y_{b,k} = \left\{ y_{b,k}^{(i)} \right\}$ and $Z_{b,k} = \left\{ z_{b,k}^{(i)} \right\}$, $i = 1,\ldots,J_{\gamma,k}$, we obtain the birth target components $\left(m_{\gamma,k}^{(i)},\ P_{\gamma,k}^{(i)} \right)$ for the next time step $k+1$ using the DI.

$$m_{\gamma,k}^{(i)} = \left[p_{\gamma,X} \quad \dot{p}_{\gamma,X} \quad p_{\gamma,Y} \quad \dot{p}_{\gamma,Y} \right]^T, \quad i = 1,\ldots,J_{\gamma,k}$$

$$\left[p_{\gamma,X} \quad p_{\gamma,Y} \right]^T = y_{b,k}^{(i)},\ \begin{bmatrix} \dot{p}_{\gamma,X} \\ \dot{p}_{\gamma,Y} \end{bmatrix} = -\beta \begin{bmatrix} \cos\theta_{b,k}^{(i)} \\ \sin\theta_{b,k}^{(i)} \end{bmatrix} d_{b,k}^{(i)},$$

$$z_{b,k}^{(i)} = \left[r_{b,k}^{(i)} \quad \theta_{b,k}^{(i)} \quad d_{b,k}^{(i)} \right]^T,$$

$$P_{\gamma,k}^{(i)} = \begin{bmatrix} \sigma_X^2 & 0 & \sigma_{XY}^2 & 0 \\ 0 & \sigma_{\dot{X}}^2 & 0 & \sigma_{X\dot{Y}}^2 \\ \sigma_{XY}^2 & 0 & \sigma_{\dot{Y}}^2 & 0 \\ 0 & \sigma_{X\dot{Y}}^2 & 0 & \sigma_{\dot{Y}}^2 \end{bmatrix},\ R_{C,k}^{(i)} = \begin{bmatrix} \sigma_X^2 & \sigma_{XY}^2 \\ \sigma_{XY}^2 & \sigma_{\dot{Y}}^2 \end{bmatrix}$$

$$\sigma_X^2 = (1-\beta)\cos\theta_{b,k}^{(i)}, \quad \sigma_{\dot{Y}}^2 = (1-\beta)\sin\theta_{b,k}^{(i)}$$

$$\sigma_{X\dot{Y}}^2 = -\beta\cos\theta_{b,k}^{(i)}\sin\theta_{b,k}^{(i)}, \quad \beta = \frac{\sigma_s^2}{\sigma_s^2 + \sigma_d^2} \quad (19)$$

where the corrected converted measurement error covariance $R_{C,k}^{(i)}$ obtained based on $\theta_{b,k}^{(i)}$, $r_{b,k}^{(i)}$, σ_r^2 and σ_θ^2 using [20, eq. (7a-7c)]. The prior speed error covariance σ_s^2 is given.

V. Simulation

To verify the accuracy performance of the GMPHD-I-DI filter, we compare it with GMPHD-I filters (i.e., GMPHD-OSI and GMPHD-TSI) through an MTT simulation scenario. We used a performance evaluation metric called the optimal subpattern assignment (OSPA) distance, which is specialized for the MTT filter accuracy test [21]. Since the OSPA distance calculates the localization and cardinality distance of MTT filters, the filter performance can be analyzed based on two physical aspects [21]; we selected OSPA parameters, $p = 1$ and $c = 50$ m.

For this task, we consider a simulation scenario having five targets. Target 1, 2, and 3 appear at $k = 3$, $k = 5$ and $k = 7$ and disappear at $k = 65$, $k = 68$ and $k = 71$, respectively; target 4 and 5 appear at $k = 10$ and $k = 15$, respectively and continue to exist during the whole simulation. The initial states, appearance and disappearance of each target are described in Table I. The detection range is set by the angle range $(0, 2\pi)$ and the distance range $(0,1000)\,m$. True trajectories are made by GMTI model [16], [19], as depicted in Fig. 1. For filter model parameters, the GMTI transition matrix F and the modeling error covariance Q are given by

$$F = \text{diag}\,(F_1, F_1),\ F_1 = \begin{bmatrix} 1 & T \\ 0 & 1 \end{bmatrix}$$

and

$$Q = \text{diag}\,(Q_1, Q_1),\ Q_1 = \sigma_w^2 \begin{bmatrix} \frac{T^3}{3} & \frac{T^2}{2} \\ \frac{T^2}{2} & T \end{bmatrix}$$

where $\sigma_w = 0.1$ and the sampling time $T = 1$. In addition, the measurement error standard deviations are $\sigma_\theta = 2^\circ$, $\sigma_r = 20$ m and $\sigma_d = 0.5\ \frac{\text{m}}{\text{s}}$ and the probability of target detection and target survival are $p_D = 0.9$ and $p_S = 0.95$ respectively. Clutters are assumed to be uniformly distributed in the detection region. The clutter intensity in polar coordinates is $\kappa\,(y_C) = \frac{m_c}{V} = \frac{20}{(2\pi\times 1000)=} 0.0032$. Because polar measurements are translated to Cartesian coordinates in the filters, the clutter intensity is also approximately translated to Cartesian coordinates. Thus, the translated clutter intensity is $\kappa\,(y_C) = \frac{m_c}{V} = \frac{20}{(\pi\times 500^2)} = 2.55\times 10^{-5}$, where the volume V is circle area. The maximum target speed is $v_{\max} = 35$; so the Doppler clutter intensity is $c\,(z_d) = \frac{1}{70}$. Parameters for initialization step are a distance value $\tau = \sigma_r$, initial birth target weight $w_{\gamma,k-1}^{(j)} = 0.05$ and a prior speed standard deviation $\sigma_s = 17\ \frac{\text{m}}{\text{s}}$.

We run 1000 Monte Carlo trials for each filter to obtain the OSPA distance. Figs. 2–4 present a performance comparison of the three filters: 1) GMPHD-OSI: a combination of GMPHD and OSI without DI; 2) GMPHD-TSI: a combination of GMPHD and TSI without DI; and 3) GMPHD-I-DI: a combination of GMPHD-DI and OSI with DI. The

TABLE I
Description of Initial Target States

Target Index	Initial States	Appearing Time Step	Disappearing Time Step
1	$x_0^{(1)} = [500 \quad -11 \quad 400 \quad -5]^T$	3	65
2	$x_0^{(2)} = [450 \quad -15 \quad 8 \quad 5]^T$	5	68
3	$x_0^{(3)} = [0 \quad -2 \quad 150 \quad -10]^T$	7	71
4	$x_0^{(4)} = [600 \quad -5 \quad 200 \quad 10]^T$	10	-
5	$x_0^{(5)} = [-100 \quad 12 \quad -150 \quad 2]^T$	15	-

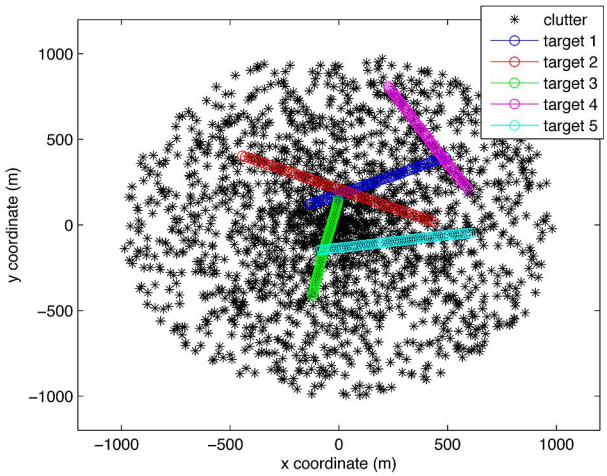

Fig. 1. Trajectories of true targets and clutters (black).

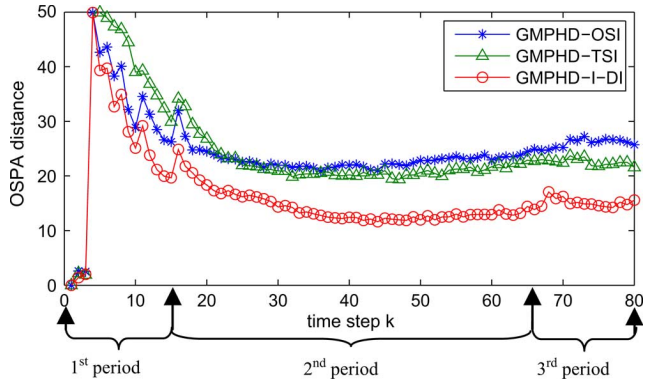

Fig. 2. OSPA distance comparison. First period: Appearance of five targets. Second period: Consistent number of targets. Third period: Disappearance of three targets.

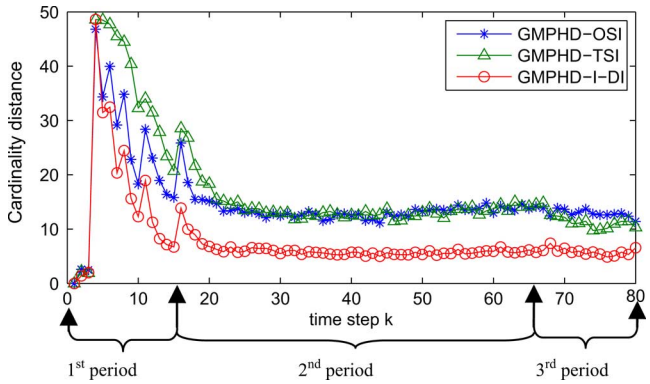

Fig. 3. Cardinality distance comparison. First period: Appearance of five targets. Second period: Consistent number of targets. Third period: Disappearance of three targets.

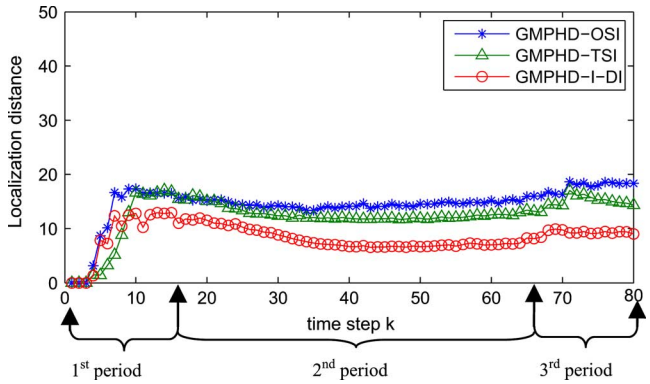

Fig. 4. Localization distance comparison. First period: appearance of five targets. Second period: consistent number of targets. Third period: Disappearance of three targets.

simulation results are analyzed over three periods: 1st period: appearance of new targets, $k \in [3,\ 15]$; 2nd period: number of targets is consistent, $k \in [16, 64]$; and 3rd period: disappearance of existing targets, $k \in [65,\ 80]$. As can be seen in Fig. 2, the OSPA distance is negligibly small at $k \in [0, 3]$ because at the beginning of operation the sets of true X_k and estimated $\hat{X}_k$ multi-target states are empty (i.e., targets do not appear and disappear).

A. Simulation Comments for First Period

We see that the cardinality distance for three filters is more dominant than the localization distance because these filters take a few time steps to confirm the appearance of new targets in Figs. 3 and 4. As shown in Fig. 3, the cardinality difference in first period between the set of estimated target states and the set of reference target states is larger than the other periods and the spikes represent the appearance of new targets. The cardinality distance of the GMPHD-I-DI filter decreases faster than other filters because DI provides more accurate information for birth targets in the initialization step.

B. Simulation Comments for Second Period

In the second period, the cardinality distance is almost constant and similar for all filters because there is no target appearance and disappearance. For this reason, the comparison of the localization distance of the three filters are distinctive as given in Fig. 4 from $k = 16$ to $k = 64$. The localization distance comparison shows that GMPHD-I-DI also performs best in accuracy.

C. Simulation Comments for 3rd Period

After $k > 65$, even though targets disappear, the accuracy performance of GMPHD-I-DI remains the best. The OSPA distances for three filters are seen to slightly increase because targets sequentially disappear at $k = 65, 68, 71$. Each time step a target disappears, the cardinality distances fluctuate a little; whereas the localization distance increases. This is because sometimes there are losses of tracks and OSPA metric automatically replaces those failures as the cut-off value, $c = 50$ which is relatively larger than the error computed from the true tracks. This track loss happens for all sequences and this loss significantly affects the localization distance when the number of targets decreases.

Remark 3: We also simulated and compared our method with the standard GMPHD update based on augmented measurements. From the result we confirmed that our method is slightly better than the standard GMPHD as described in Section III.

VI. Conclusion

In this correspondence, we associated the initialization step with GMPHD to jointly initialize and track multiple moving objects. In addition, we incorporated DI into GMPHD in order to accurately select the components of birth target intensities and correct predicted target intensities. We proposed to incorporate the DI into GMPHD using a three-step procedure, including a target state correction based on position measurements $y_{C,k} \in Y_{C,k}$ and DI $d_k \in D_k$ and update of the corresponding weights $w_k^{(j)}(z_{C,k})$ by $Z_{C,k}$. Furthermore, we added a preliminary process before the initialization methods (e.g., OSI, TSI) in GMPHD to achieve more efficient track initiation. Through a series of Monte Carlo simulations, we found that the DI significantly enhanced the filter performance in terms of its ability to estimate the states and the number of targets. For the intuitive extension of our work, our proposed method also can be applied to the Cardinalized PHD filter [23], [24] and similar performance improvements are expected.

Acknowledgment

The authors are grateful to the anonymous reviewers and Prof. B.-N Vo for their valuable comments which significantly helped to improve this correspondence.

References

[1] S. Blackman and R. Popoli, *Design and Analysis of Modern Tracking Systems*. Norwood, MA: Artech House, 1999.
[2] Y. Bar-Shalom and X. R. Li, *Multitarget-Multisensor Tracking: Principles and Techniques*. Storrs, CT: YBS Publishing, 1995.

[3] R. P. S. Mahler, *Statistical Multisource-Multitarget Information Fusion*. Norwood, MA: Artech House, 2007.
[4] S. Blackman, "Multiple hypothesis tracking for multiple target tracking," *IEEE Aerosp. Electron. Syst. Mag.*, vol. 19, no. 1, pp. 5–18, 2004.
[5] D. Mušicki, R. Evans, and S. Stankovic, "Integrated probabilistic data association," *IEEE Trans. Autom. Control*, vol. 39, no. 6, pp. 1237–1241, 1994.
[6] D. Mušicki and R. Evans, "Joint integrated probabilistic data association: JIPDA," *IEEE Trans. Aerosp. Electron. Syst.*, vol. 40, no. 3, pp. 1093–1099, 2004.
[7] D. Mušicki, B. L. Scala, and R. J. Evens, "Multi-target tracking in clutter without measurement assignment," *IEEE Trans. Aerosp. Electron. Syst.*, vol. 44, no. 3, pp. 877–896, 2008.
[8] R. Mahler, "Multitarget Bayes filtering via first-order multitarget moments," *IEEE Trans. Aerosp. Electron. Syst.*, vol. 39, no. 4, pp. 1152–1178, 2003.
[9] B. N. Vo, S. Singh, and A. Doucet, "Sequential Monte Carlo methods for multitarget filtering with random finite sets," *IEEE Trans. Aerosp. Electron. Syst.*, vol. 41, no. 4, pp. 1224–1245, 2005.
[10] B. N. Vo and W. K. Ma, "The Gaussian mixture probability hypothesis density filter," *IEEE Trans. Signal Process.*, vol. 54, no. 11, pp. 4091–4104, 2006.
[11] B. N. Vo, B. T. Vo, N. T. Pham, and D. Suter, "Joint detection and estimation of multiple objects from image observations," *IEEE Trans. Signal Process.*, vol. 58, no. 10, pp. 5129–5141, 2010.
[12] D. Lerro and Y. Bar-Shalom, "Automated tracking with target amplitude information," in *Proc. Amer. Control Conf.*, 1990, pp. 2875–2880.
[13] B. F. La Scala, "Viterbi data association tracking using amplitude information," presented at the 7th Int. Conf. Inf. Fusion, Stockholm, Sweden, Jun. 28–Jul. 1, 2004.
[14] D. Clark, B. Ristic, B. N. Vo, and B. T. Vo, "Bayesian multi-object filtering with amplitude feature likelihood for unknown object SNR," *IEEE Trans. Signal Process.*, vol. 58, no. 1, pp. 26–37, 2010.
[15] S. W. Yeom, T. Kirubarajan, and Y. Bar-Shalom, "Track segment association fine-step IMM and initialization with Doppler for improved track performance," *IEEE Trans. Aerosp. Electron. Syst.*, vol. 40, no. 1, pp. 293–309, 2004.
[16] X. Wang, D. Mušicki, R. Ellem, and F. Fletcher, "Efficient and enhanced multi-target tracking with Doppler measurements," *IEEE Trans. Aerosp. Electron. Syst.*, vol. 45, no. 4, pp. 1400–1417, 2009.
[17] D. Mušicki, "Doppler-aided target tracking in heavy clutter," presented at the 13th Int. Conf. Inf. Fusion (FUSION), Edinburgh, U.K., Jul. 26–29, 2010.
[18] Y. Bar-Shalom and G. A. Watson, "Automatic track formation in clutter with a recursive algorithm," in *Proc. 28th Conf. Decision, Control*, Dec. 1989, pp. 1402–1408.
[19] X. R. Li and V. P. Jilkov, "Survey of maneuvering target tracking. Part 1: Dynamic models," *IEEE Trans. Aerosp. Electron. Syst.*, vol. 39, no. 4, pp. 1333–1363, 2003.
[20] M. Longbin, S. Xiaoquan, Z. Yizu, Z. S. Kang, and Y. Bar-Shalom, "Unbiased converted measurements for tracking," *IEEE Trans. Aerosp. Electron. Syst.*, vol. 34, no. 3, pp. 1023–1027, 1998.
[21] D. Schuhmacher, B. T. Vo, and B. N. Vo, "A consistent metric for performance evaluation of multi-object filters," *IEEE Trans. Signal Process.*, vol. 56, no. 8, pp. 3447–3457, 2008.
[22] B. Han, Y. Zhu, D. Comaniciu, and L. S. Davis, "Visual tracking by continuous density propagation in sequential Bayesian filtering framework," *IEEE Trans. Pattern Anal. Mach. Intell.*, vol. 31, no. 5, pp. 919–930, 2009.
[23] R. Mahler, "PHD filters of higher order in target number," *IEEE Trans. Aerosp. Electron. Syst.*, vol. 43, no. 4, pp. 1523–1532, 2007.
[24] B. Vo, B. Vo, and A. Cantoni, "Analytic implementations of the cardinalized probability hypothesis density filter," *IEEE Trans. Signal Process.*, vol. 55, no. 7, pp. 3533–3567, 2007.

A Metric for Performance Evaluation of Multi-Target Tracking Algorithms

Branko Ristic, Ba-Ngu Vo, Daniel Clark, and Ba-Tuong Vo

***Abstract*—Performance evaluation of multi-target tracking algorithms is of great practical importance in the design, parameter optimization and comparison of tracking systems. The goal of performance evaluation is to measure the distance between two sets of tracks: the ground truth tracks and the set of estimated tracks. This paper proposes a mathematically rigorous metric for this purpose. The basis of the proposed distance measure is the recently formulated consistent metric for performance evaluation of multi-target *filters*, referred to as the OSPA metric. Multi-target filters sequentially estimate the number of targets and their position in the state space. The OSPA metric is therefore defined on the space of finite sets of vectors. The distinction between *filtering* and *tracking* is that tracking algorithms output *tracks* and a track represents a labeled temporal sequence of state estimates, associated with the same target. The metric proposed in this paper is therefore defined on the space of finite sets of tracks and incorporates the labeling error. Numerical examples demonstrate that the proposed metric behaves in a manner consistent with our expectations.**

***Index Terms*—Estimation, performance evaluation, tracking.**

I. Introduction

Multi-target tracking refers to the sequential estimation of the number of targets and their states (positions, velocities, etc.) tagged by a unique label. Hence, the output of a tracking algorithm are *tracks*, where a track represents a labeled temporal sequence of state estimates, associated with the same target.

In evaluating the performance of a multi-target tracking algorithm the goal is to measure the distance between two sets of tracks: the set of ground truth tracks and the set of estimated tracks, produced by the tracking algorithm under evaluation. Performance evaluation of multi-target tracking algorithms is of great practical importance, with applications in tracking system design, parameter tuning and tracker comparisons (e.g., in tender evaluations). Consequently, the topic has been studied extensively; see, for example, [1], [2], [3, Ch. 13], [4], and [5].

The general performance evaluation methodology includes three steps: 1) the creation of a scenario of a certain level of difficulty; 2) running of the multi-target tracking algorithm under assessment; and 3) assignment of a performance measure (score) as a measure of the distance between the ground truth and the tracker output. In order to estimate the expected performance, the score is typically averaged

Manuscript received November 15, 2010; revised March 03, 2011; accepted March 25, 2011. Date of publication April 07, 2011; date of current version June 15, 2011. The associate editor coordinating the review of this manuscript and approving it for publication was Dr. Mark Coates.

B. Ristic is with the Defence Science and Technology Organisation, ISR Division, Fishermans Bend, VIC 3207, Australia (e-mail: branko.ristic@dsto.defence.gov.au).

B.-N. Vo and B.-T. Vo are with the School of Electrical, Electronic, and Computer Engineering, The University of Western Australia, Crawley, WA 6009, Australia (e-mail: ba-ngu.vo@uwa.edu.au; ba-tuong.vo@uwa.edu.au).

D. Clark is with the Joint Research Institute in Signal and Image Processing, School of EPS, Heriot-Watt University, Riccarton, Edinburgh, EH14 4AS, U.K. (e-mail: D.E.Clark@hw.ac.uk).

This paper has supplementary downloadable multimedia material available at http://ieeexplore.ieee.org provided by the authors.

Color versions of one or more of the figures in this paper are available online at http://ieeexplore.ieee.org.

Digital Object Identifier 10.1109/TSP.2011.2140111